Supporting Information for

Enhanced Corneal Retention of Hyaluronic Acid *via* Metabolic Glycoengineering-based *In Vivo* Bioorthogonal Reaction

Buwei Hu[1,2], Hui Wang[6], Chenlin Ji[2,5], Xuehan Xu[2,5], Luyi Wang[2,5], Tingting Cao[2,5], Menghua Gao[2,3,4], Yanjun Zhao[7], Bin Wang[8*], Wenjing Xuan[2,3,4*], Jianjun Cheng[2,3,4*]

[1]Department of Materials Science, Fudan University, Shanghai 200433, China
[2]Department of Materials Science and Engineering, Westlake University, Hangzhou, Zhejiang 310030, China
[3]Research Center for Industries of the Future, Westlake University, Hangzhou, Zhejiang 310030, China
[4]Institute of Advanced Technology, Westlake Institute for Advanced Study, Hangzhou, Zhejiang 310024, China
[5]School of Material Science and Engineering, Zhejiang University, Hangzhou, Zhejiang 310023, China
[6]School of Science, Westlake University, Hangzhou, Zhejiang 310030, China
[7]Tianjin Key Laboratory for Modern Drug Delivery & High Efficiency, School of Pharmaceutical Science & Technology, Faculty of Medicine, Tianjin University, Tianjin 300072, China
[8]Department of Ophthalmology, Tongde Hospital of Zhejiang Province, Hangzhou, Zhejiang 310012, China

[*]Corresponding author.
E-mail: chengjianjun@westlake.edu.cn; xuanwenjing@westlake.edu.cn; zjsltdyk@163.com

Figure Legend

Figure S1: Characterization of DBCO decorated hyaluronic acid.

Figure S2: Representative contact angle illustration of HA with different DBCO conjugation degree.

Figure S3: Western blot analysis of HCEC cell line azide glycol labelling for different days.

Figure S4: HCEC azide labelling AAM concentration-dependent kinetic analysis.

Figure S5: HCEC cytotoxicity analysis of AAM.

Figure S6: DBCO-Cy5 reaction kinetics on HCEC.

Figure S7: Biocompatibility of HA with different DBCO decoration percentages.

Figure S8: HA-$DBCO_{0\%}$-Cy5 time and concentration-dependent Click reaction kinetics on HCEC treated with or without AAM.

Figure S9: HA-$DBCO_{0\%}$-Cy5 and HA-$DBCO_{4\%}$-Cy5 concentration-dependent Click reaction-based HCEC attachment enhancement.

Figure S10: DOTAP and DOPC-AAM liposome characterization.

Figure S11: Western blot analysis of mouse eyes treated with different AAM formulation.

Figure S12: Western blot analysis of mouse eyes treated with DOTAP formulation for different days.

Figure S13: Western blot analysis of azide sustain time for different days after AAM labelling.

Figure S14: HA-$DBCO_{4\%}$ corneal retention after eyeballs treated with AAM liposome for different days.

Figure S15: Western blot analysis of azide label efficiency on the dry eye disease model.

Figure S16: Western blot analysis of azide label efficiency on the dry eye disease model original data.

Figure S17: Analysis of reactive oxygen species (ROS) and inflammatory factors *via* immunofluorescence in dry eye disease treatment.

Figure S18: Therapeutic evaluation of AAM-loaded liposomes in dry eye disease.

Figure S19: Dry eye disease treatment biocompatibility analysis.

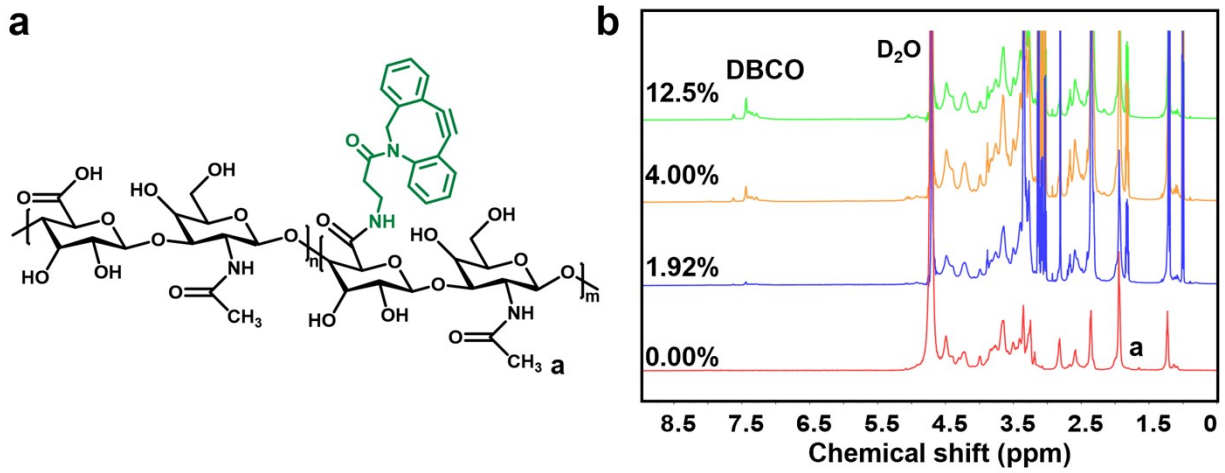

Figure S1. Characterization of DBCO decorated hyaluronic acid. a) The chemical structure of DBCO-decorated hyaluronic acid; b) ^{1}HNMR of HA with different DBCO conjugation degree in D_2O.

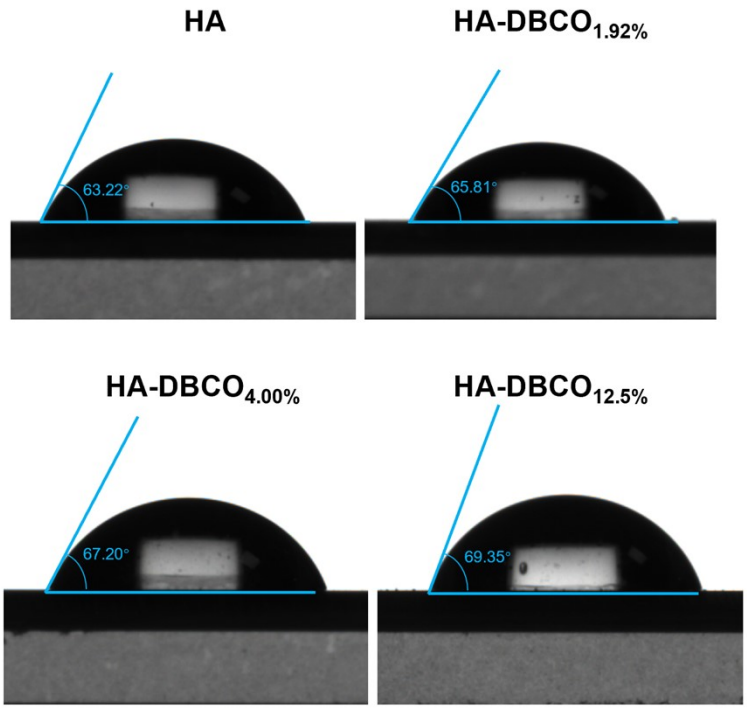

Figure S2. Representative contact angle illustration of HA with different DBCO conjugation degree.

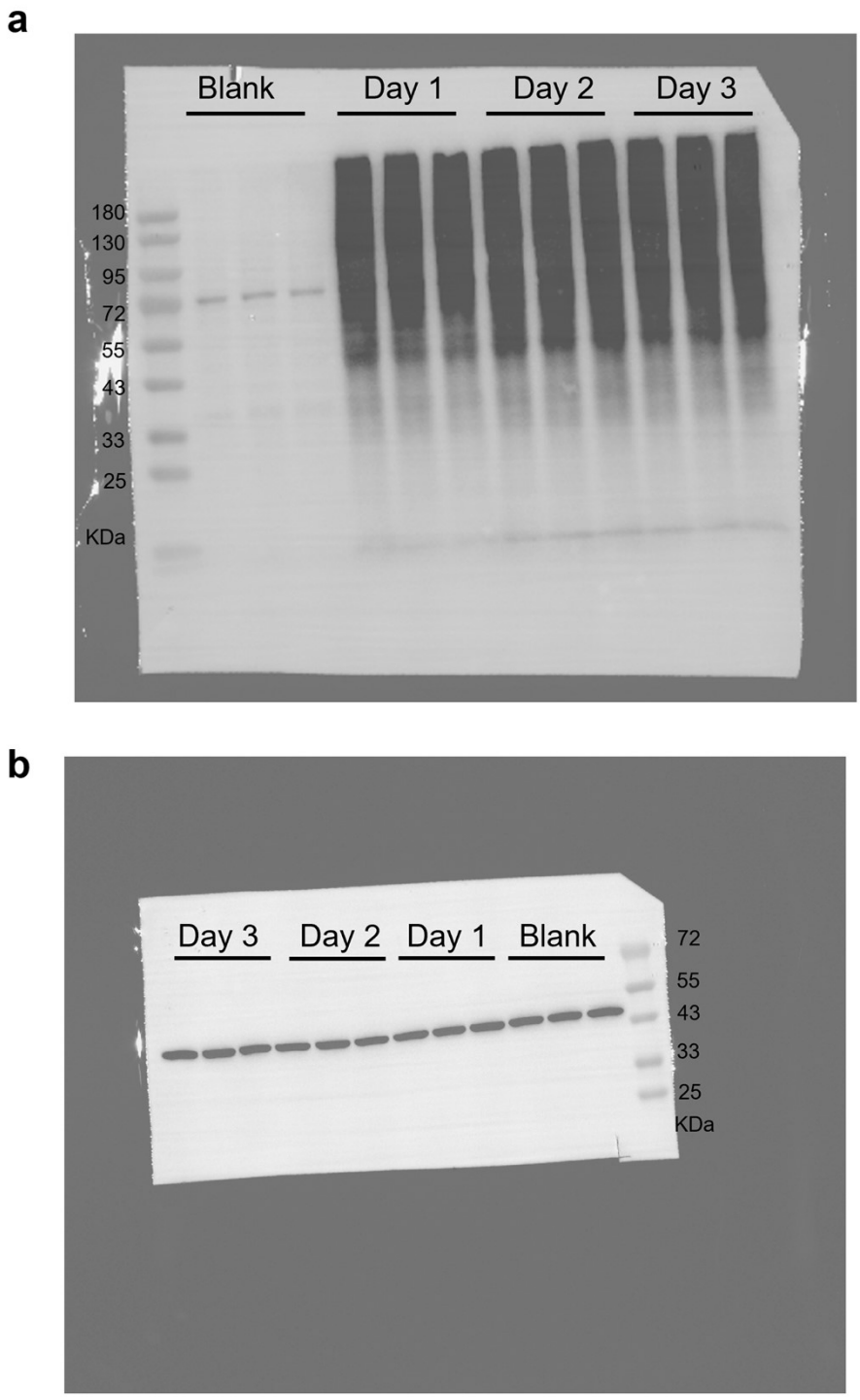

Figure S3. Western blot analysis of HCEC cell line azide glycol labelling for different days. a) Azide glycol labelling result; b) Actin of corresponding sample.

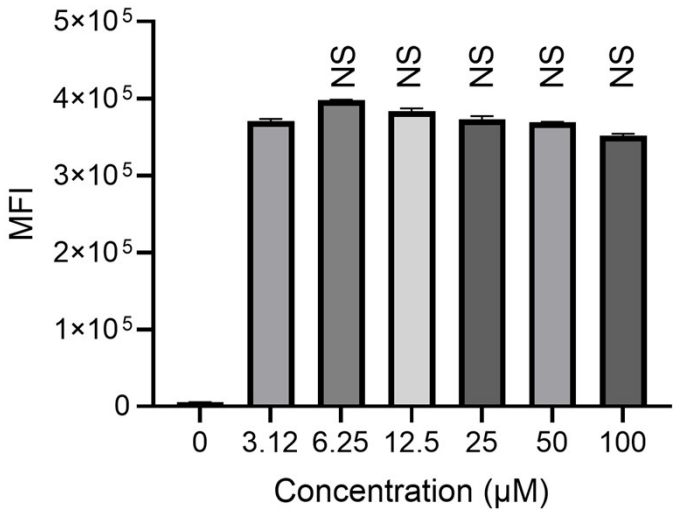

Figure S4. HCEC azide labelling efficiency after treated with different AAM concentration medium for 1 day. The statistical analysis was made with reference to 3.12 μM group. (n = 3, NS, no significant difference).

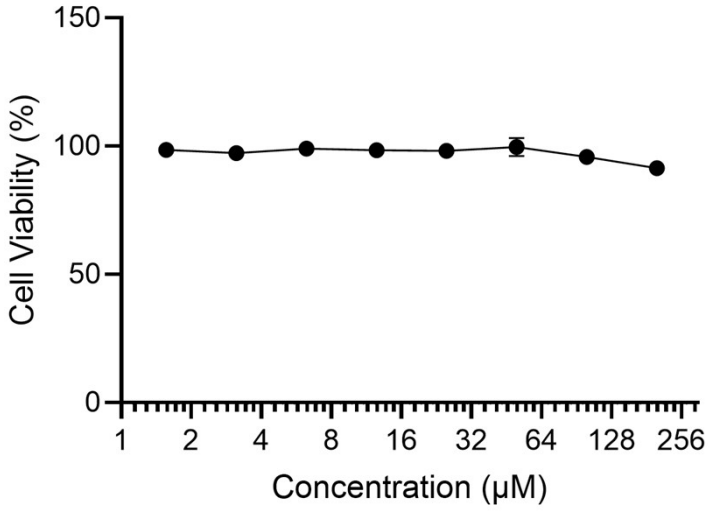

Figure S5. HCEC cytotoxicity analysis of different AAM concentration treatment for 1 day (*n* = 3).

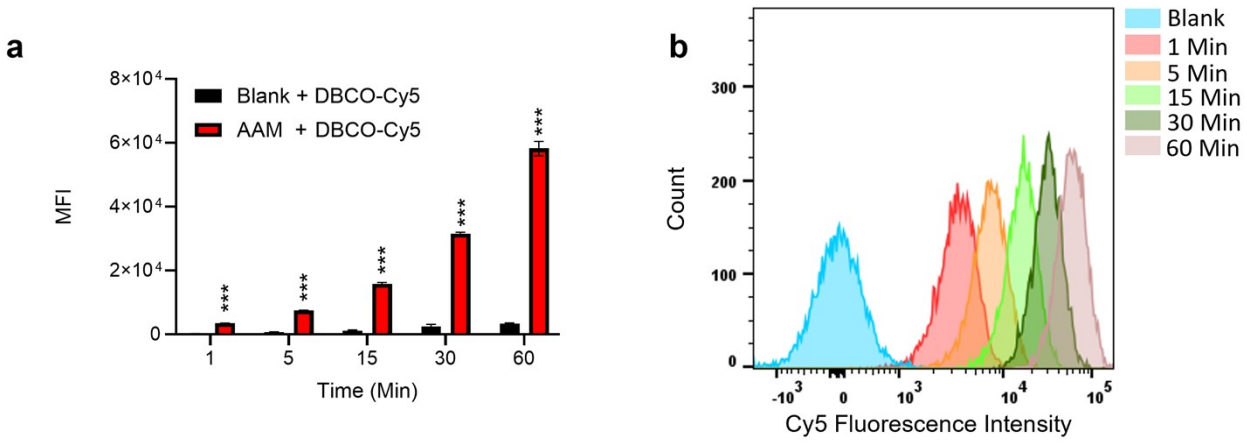

Figure S6. DBCO-Cy5 reaction kinetics on HCEC treated with or without AAM. a) Statistical analysis of flowcytometry results; b) The time-dependent kinetic of DBCO-Cy5 reaction on azide labelled HCEC. The statistical analysis was made with reference to blank group (n = 3, ***p < 0.001).

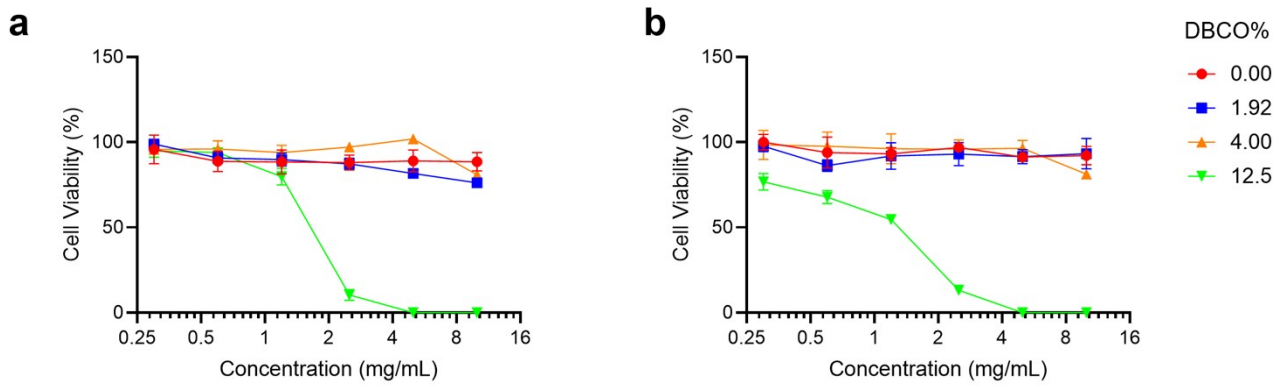

Figure S7. Biocompatibility of HA with different DBCO decoration percentage. Cytotoxicity analysis of HA decorated with different DBCO percentage, a) Blank HCEC; b) Azide labelled HCEC (n = 3).

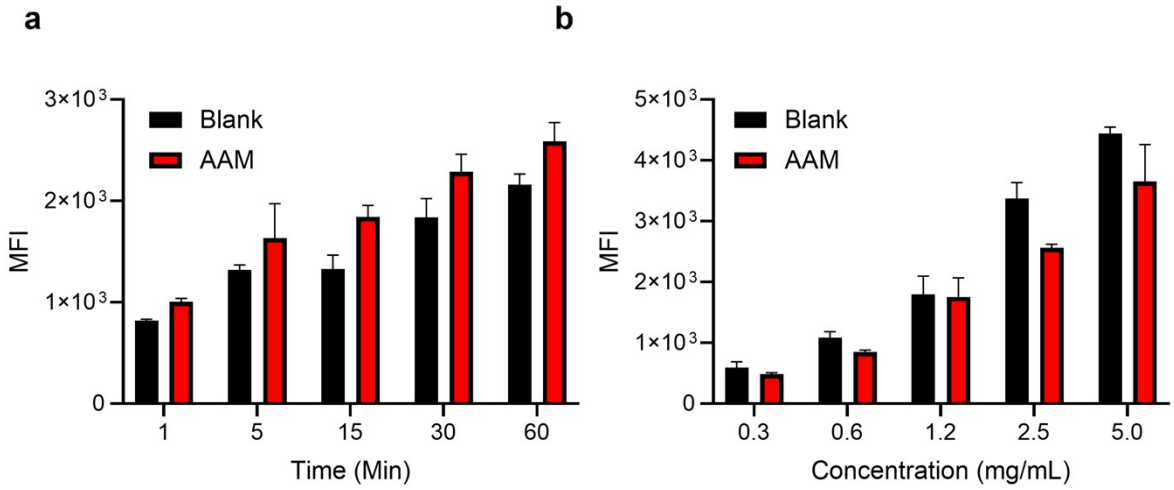

Figure S8. HA-DBCO$_{0\%}$-Cy5 a) Time (1 mg/mL) and b) Concentration-dependent kinetic on HCEC treated with or without AAM (n = 3).

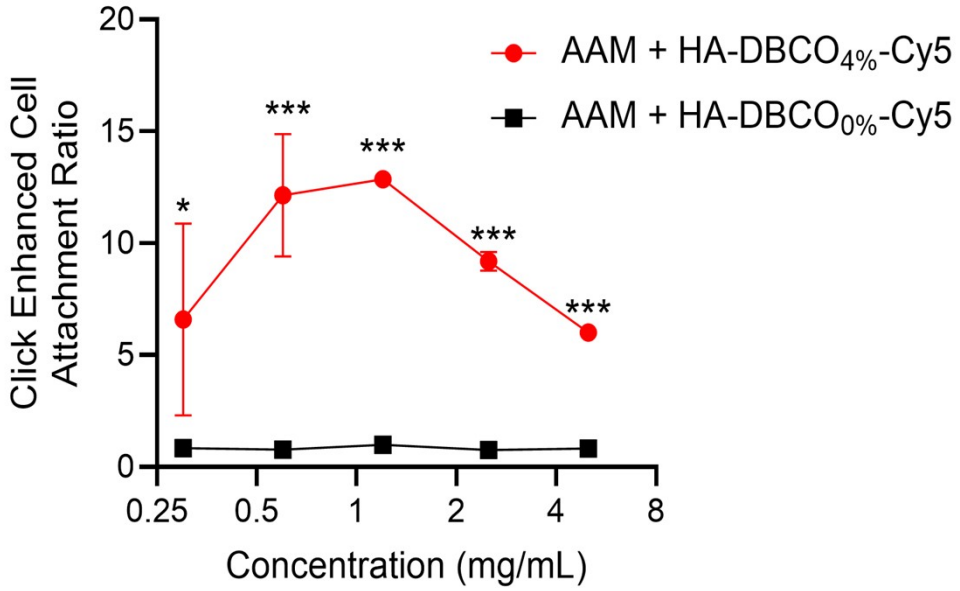

Figure S9. HA-$DBCO_{0\%}$-Cy5 and HA-$DBCO_{4\%}$-Cy5 Click reaction-based HCEC surface enhanced attachment under different concentration. The statistical analysis was made with reference to AAM + HA-$DBCO_{0\%}$ group (*$p < 0.05$, ***$p < 0.001$, $n = 3$).

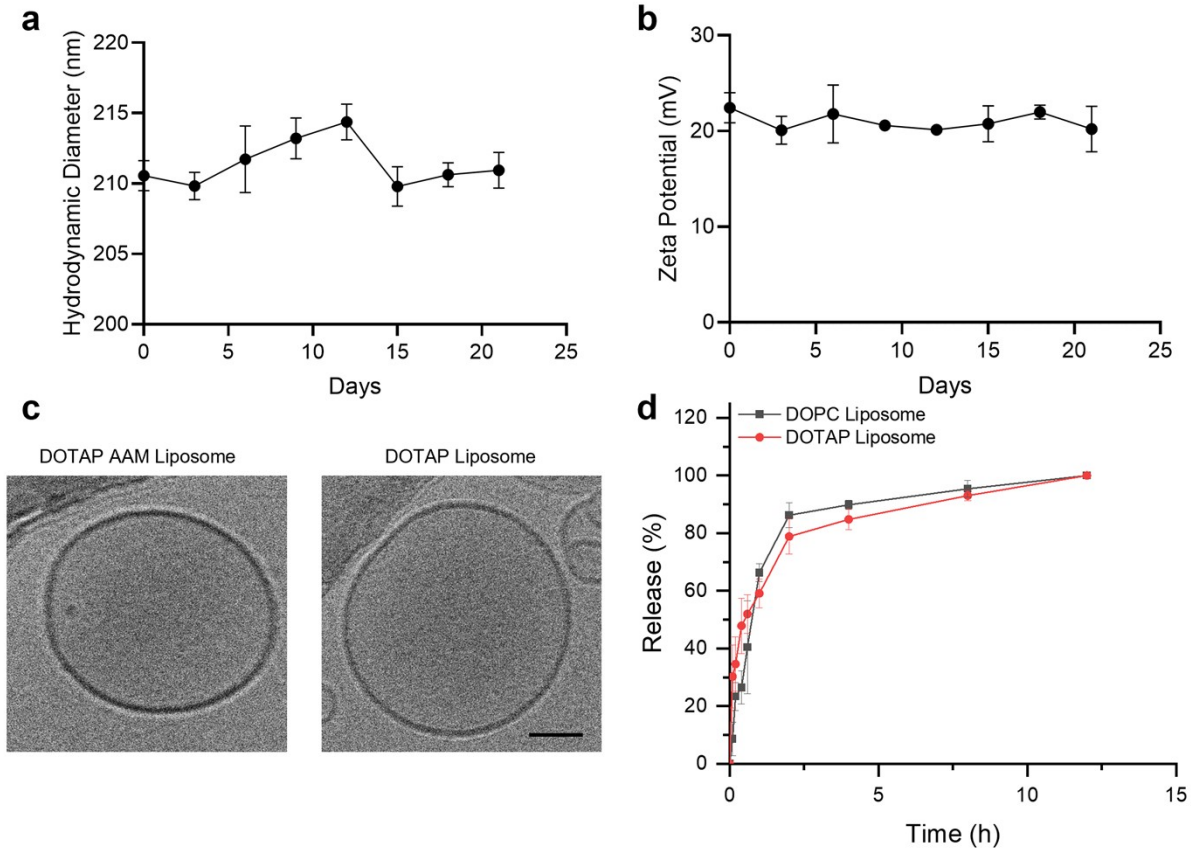

Figure S10. DOTAP and DOPC AAM liposome characterization. a) Hydrodynamic diameter of DOTAP AAM liposome after preserved at 4℃ for different days (n = 3); b) Zeta potential of DOTAP AAM liposome after preserved at 4℃ for different days; c) Cryo-EM image of DOTAP liposome with or without AAM loading. Scale bar: 50 nm; d) Analysis of AAM release kinetics of DOTAP and DOPC AAM liposome (n = 3).

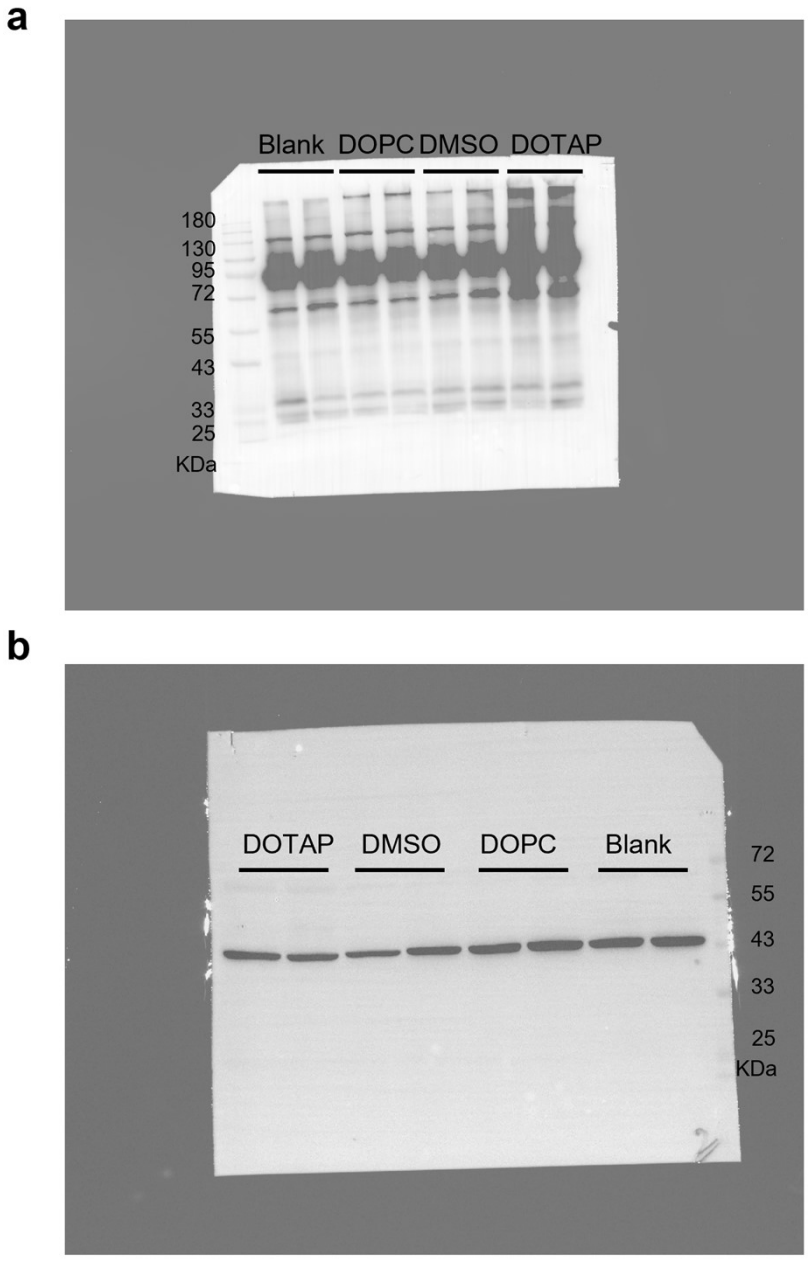

Figure S11. Western blot analysis of mouse eye being treated with different AAM formulation. a) Azide glycol labelling result; b) Actin of corresponding sample.

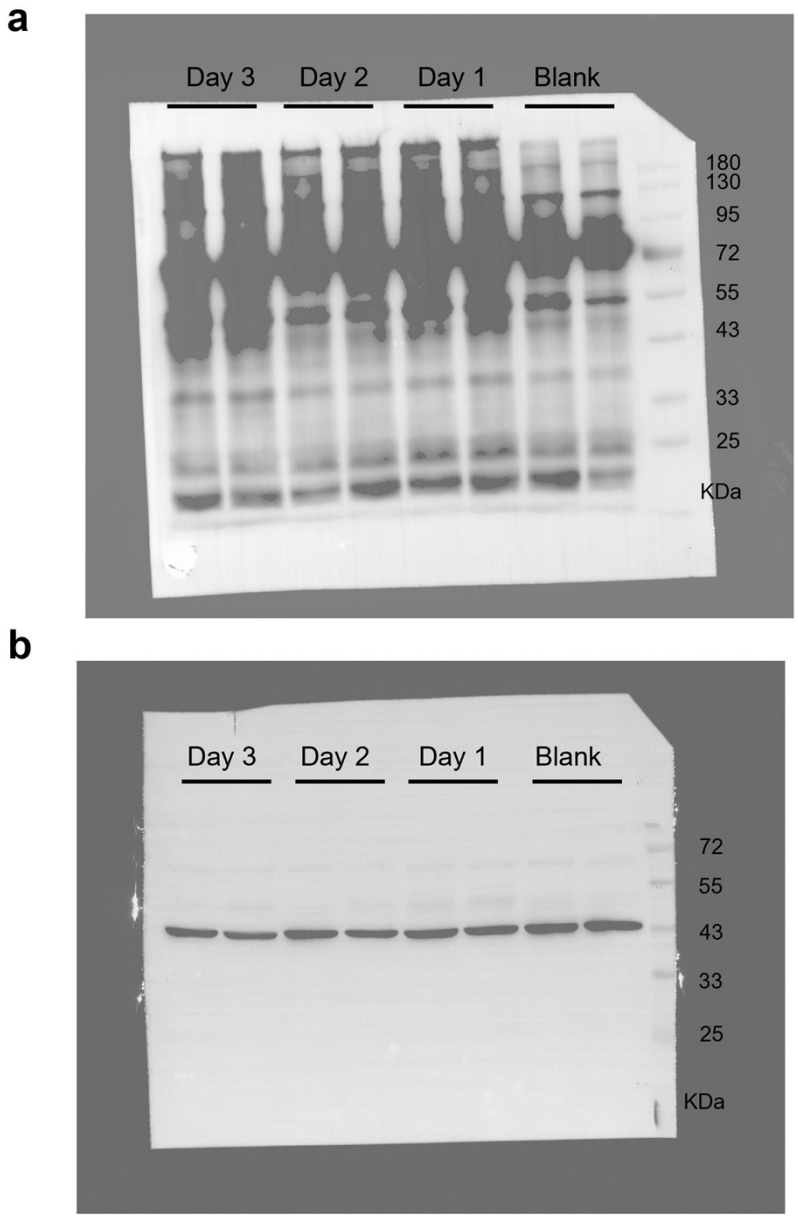

Figure S12. Western blot analysis of mouse eyes being treated with DOTAP formulation for different days. a) Azide glycol labelling result; b) Actin of corresponding sample.

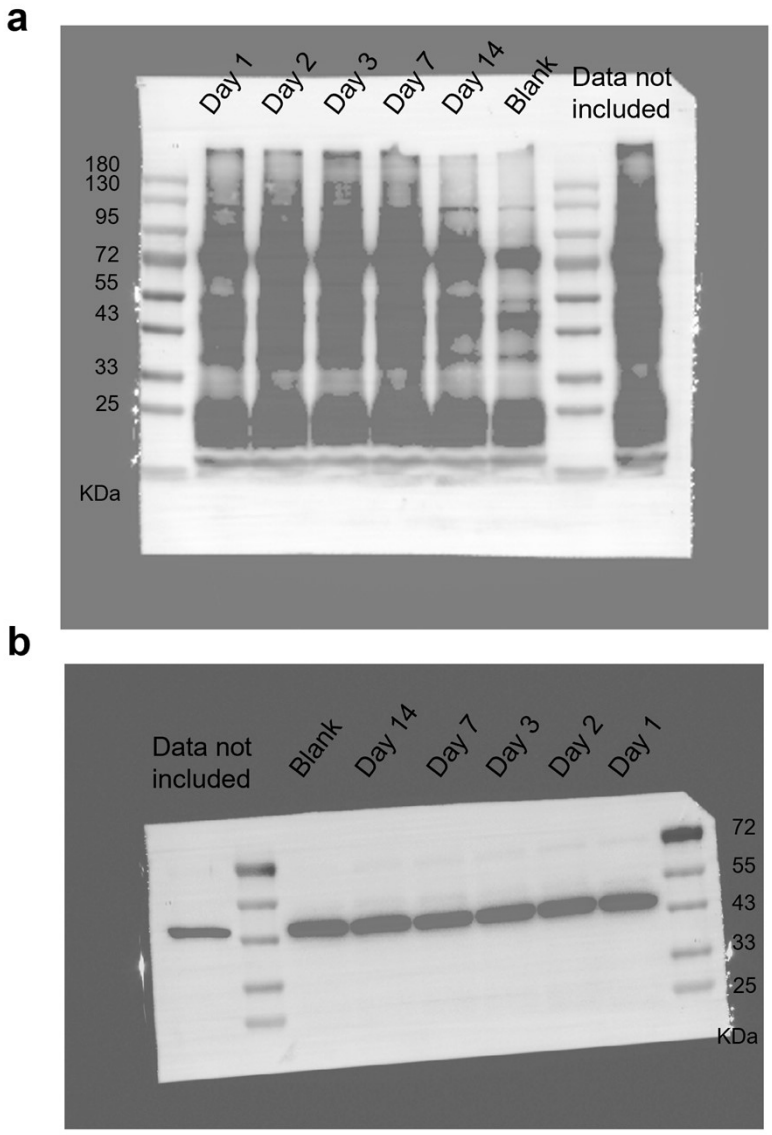

Figure S13. Western blot analysis of azide sustain time for different days after two days AAM topical administration. a) Azide glycol labelling result; b) Actin of corresponding sample.

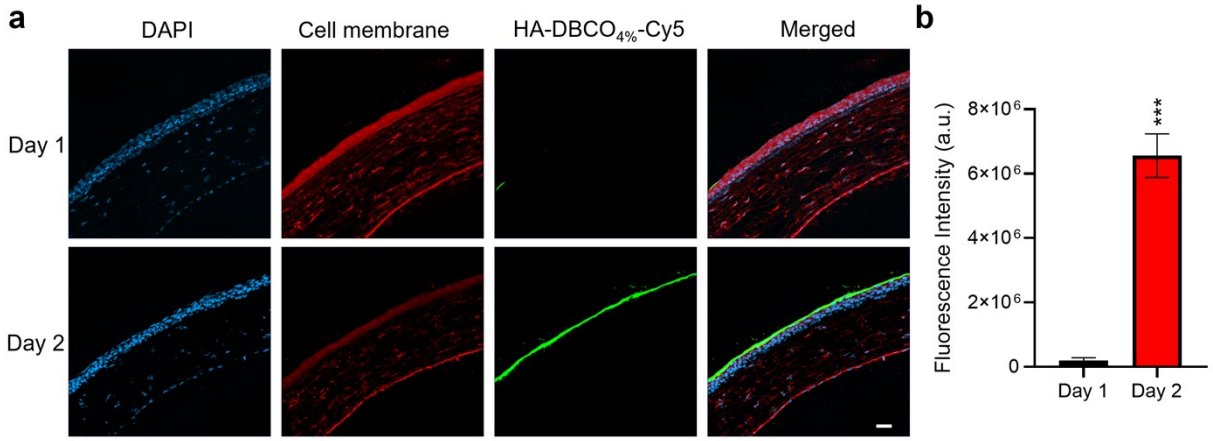

Figure S14. HA-DBCO$_{4\%}$-Cy5 cornea retention after mouse eyes treated with DOTAP AAM liposome for different days. a) CLSM image of HA-DBCO$_{4\%}$-Cy5 on cornea after treated with DOTAP AAM liposome for 1 or 2 days; b) Semiquantitative analysis of Cy5 retained on cornea in (a) obtained by ImageJ software. Scale bar: 20 μm. The statistical analysis was made with reference to day 1 group (n = 3, ***p < 0.001).

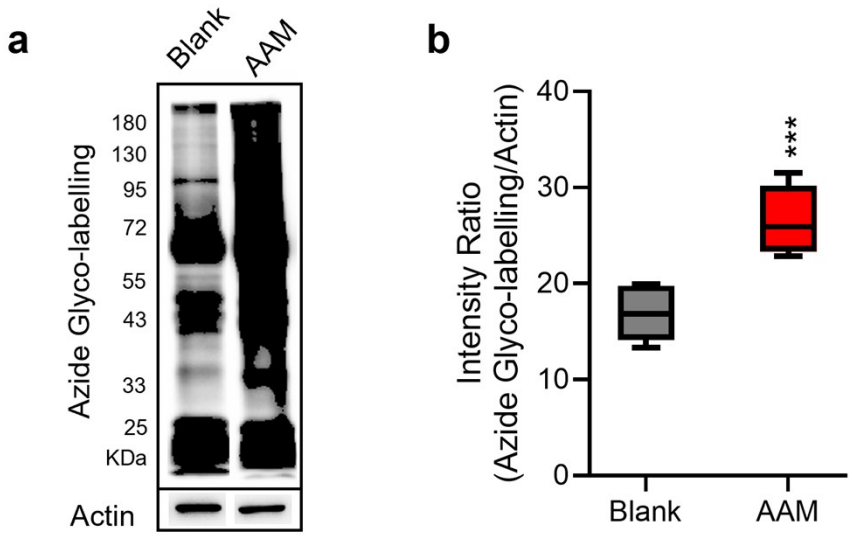

Figure S15. Western blot analysis of azide labelling efficiency on the dry eye disease model. a) Western blot analysis of dry eye disease azide labelling efficiency and b) Corresponding statistical analysis. The statistical analysis was made with reference to blank group. ($n = 6$, ***$p < 0.001$).

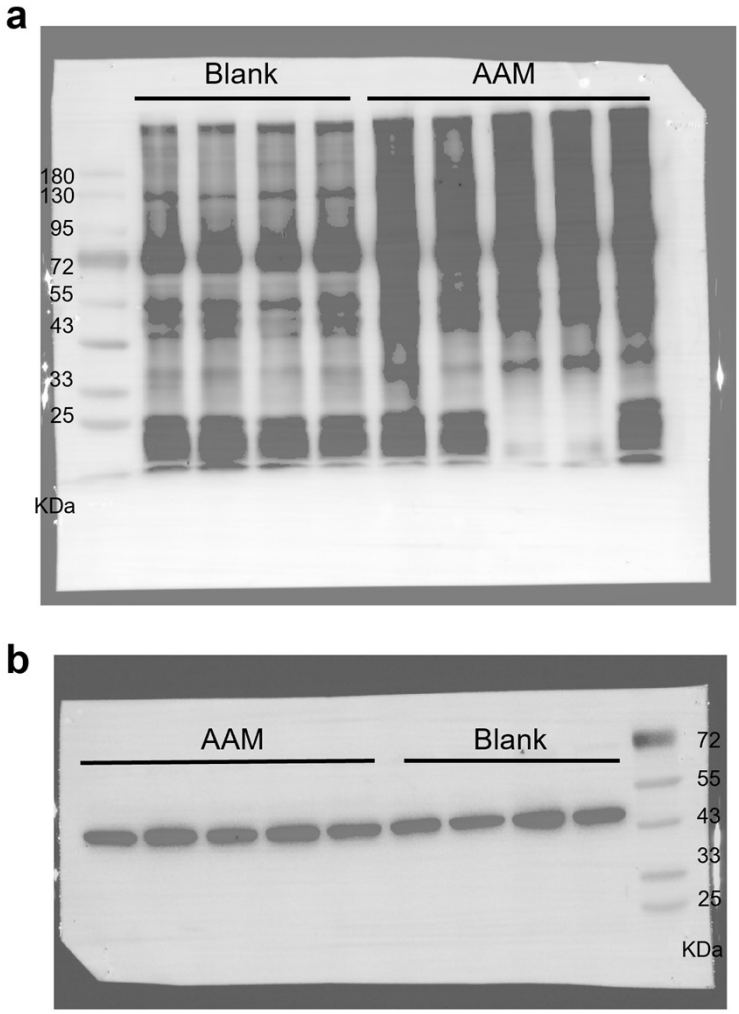

Figure S16. Western blot analysis of azide labelling efficiency on dry eye disease model after two days topical administration. a) Azide glycol labelling result; b) Actin of corresponding sample.

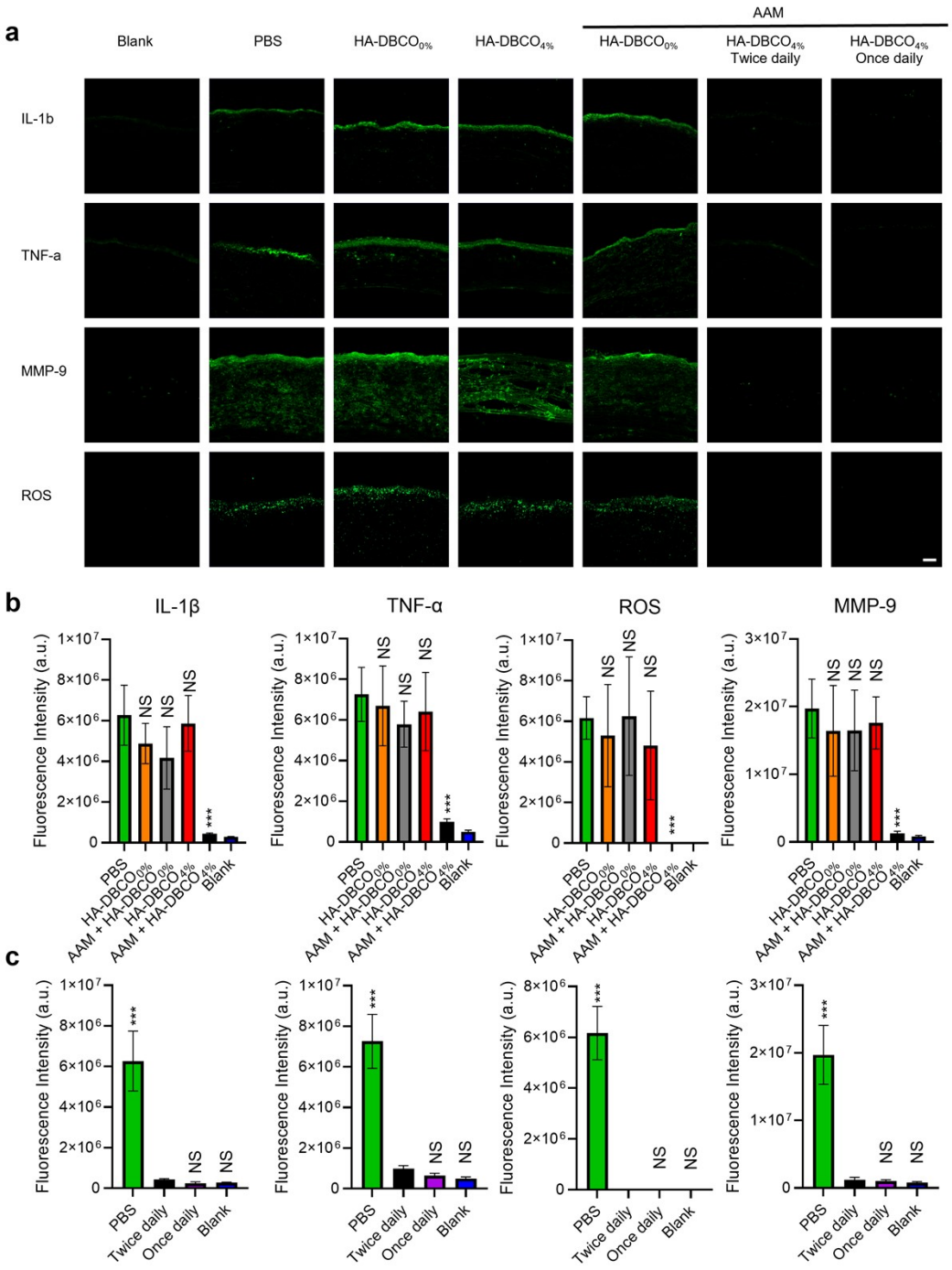

Figure S17. Analysis of reactive oxygen species (ROS) and inflammatory factors *via* immunofluorescence in dry eye disease treatment. a) Representative images of inflammatory factors (IL-1β, TNF-α), matrix-degrading enzyme (MMP-9) and ROS fluorescence staining of each treatment group in DED treatment analysis, scale bar: 50 μm; Semiquantitative analysis of fluorescence intensity of inflammatory factors obtained by ImageJ software of b) Ocular surface Click reaction enhanced HA retention for inflammatory factors reduction (n = 5). The statistical analysis was performed with reference to PBS group, and c) Inflammatory factors reduction efficacy of different HA-$DBCO_{4\%}$ administration frequency (n = 5). Statistical analysis was performed with reference to twice daily group (***$p < 0.001$. NS, no significant difference).

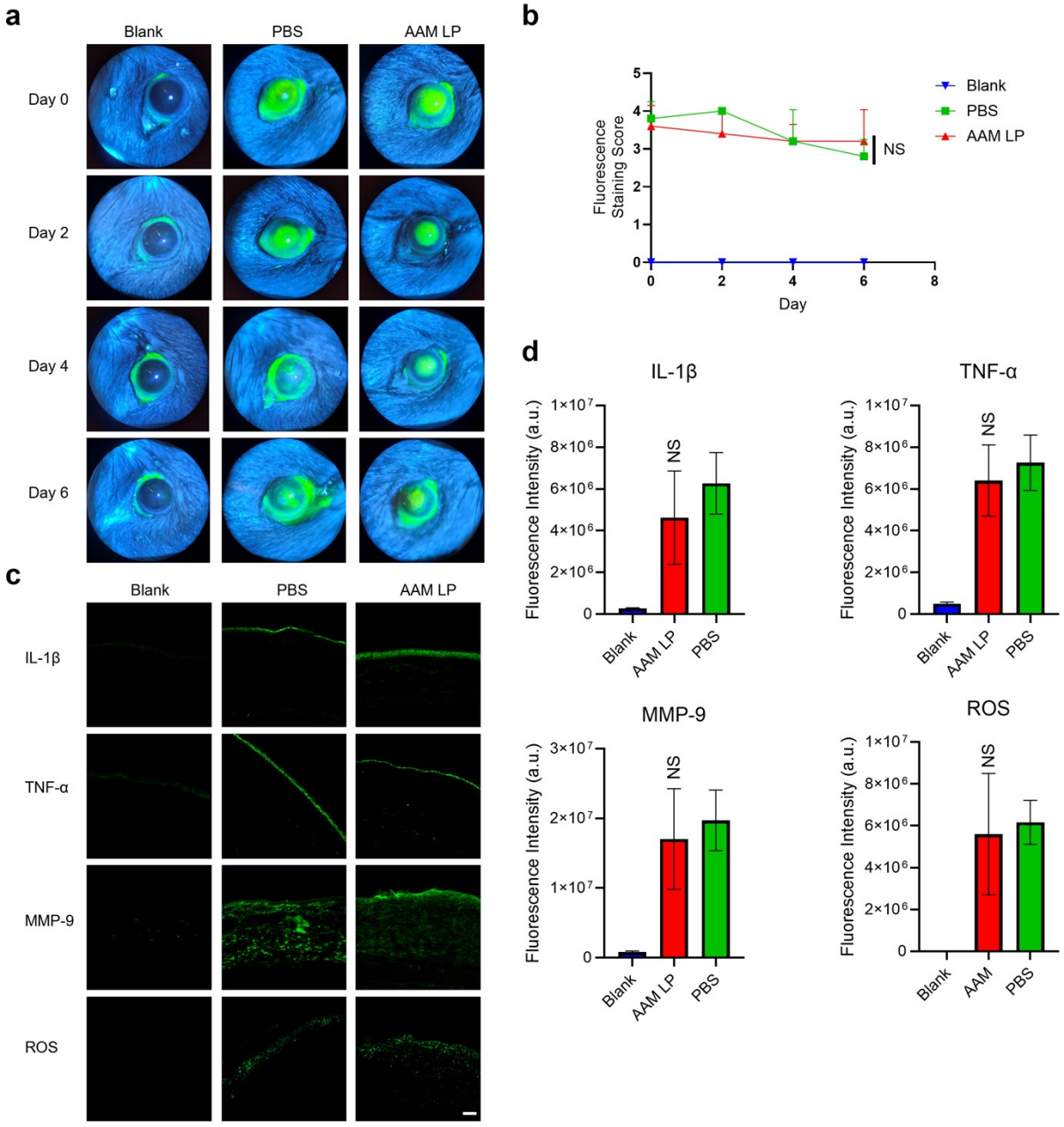

Figure S18. Therapeutic evaluation of AAM-loaded liposomes in dry eye disease. a) Representative fluorescein sodium staining images (green color when photographed with Cobalt blue filter) and b) The corresponding staining scores for the fluorescein sodium staining (n = 5); c) Representative images of inflammatory factors (IL-1β, TNF-α), matrix-degrading enzyme (MMP-9) and ROS fluorescence staining, scale bar: 50 μm; and d) The Semiquantitative analysis of fluorescence intensity of inflammatory factors obtained by ImageJ software (n = 5). All statistical analysis was performed with reference to PBS group. LP, liposome; NS, no significant difference).

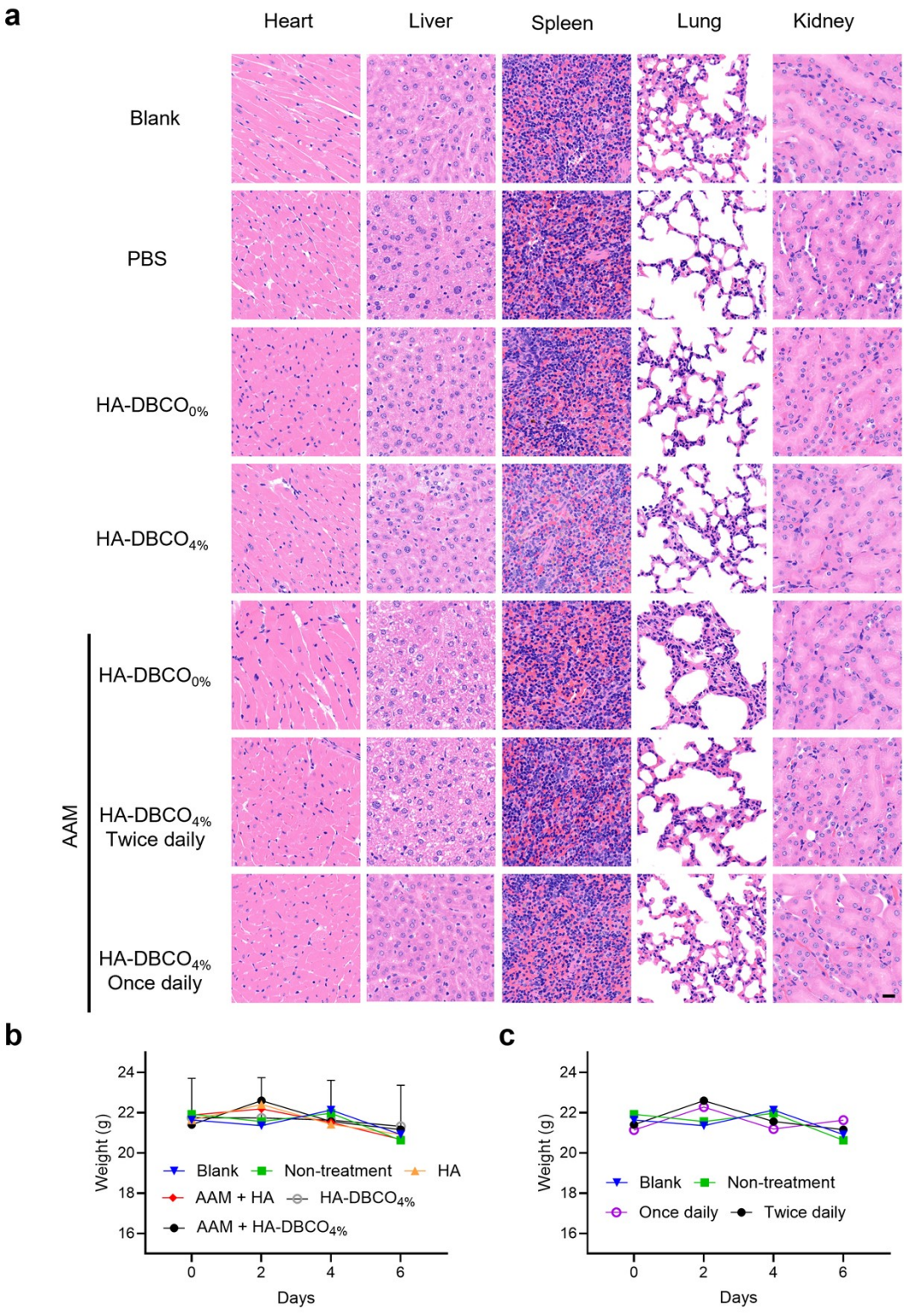

Figure S19. Dry eye disease treatment biocompatibility analysis. a) H&E staining of the primary organ (heart, liver, spleen, lung and kidney) on day 6 after topical administration treatment; b) Body weight change during ocular surface Click mediated dry eye disease treatment and c) Body weight change with different HA-DBCO$_{4\%}$ administration frequency (n = 5). Scale bar: 20 μm.